2008 10th Intl. Conf. on Control, Automation, Robotics and Vision
Hanoi, Vietnam, 17–20 December 2008

Synthesis and Comparison of Fine Actuator Controllers for a 3-DOF Micro Parallel Positioning Platform

Tae Won Seo, Deuk Soo Kang and Jongwon Kim
School of Mechanical and Aerospace Engineering
Seoul National University
Seoul, Korea
seotw@rodel.snu.ac.kr

***Abstract*—This paper presents the controller synthesis for a fine actuation system of a 3-DOF micro parallel positioning platform. The platform is composed of a dual stage servo system for realizing both long stroke and high precision, simultaneously. Among the dual stage, the fine actuation system is more important as it guarantees high speed and accuracy. First, a physics-based model for the fine actuation system is developed through the constraint equations of the parallel mechanism and the dynamic equations of the fine actuation system. Several experiments have been conducted and unknown physical parameters such as the stiffness and the damping coefficients were estimated to precisely predict the dynamics of the fine actuation system. Equipped with the physics-based model, the PID-based controller, mixed-sensitivity H_2 and H_∞ controllers were designed to accomplish both high accuracy and fast response of the micro positioning platform, respectively. The satisfactory performances of the synthesized controllers were successfully verified and compared with one another through extensive simulations and experiments.**

***Keywords*—precision control, robust control, micro parallel mechanism, system identification**

I. INTRODUCTION

Parallel mechanism consists of a fixed platform, a movable platform and links that are connecting the two platforms. Parallel mechanism machines are being researched in industry fields since the mechanism machines have some advantages in small scale movement such as high resolution, low moving mass, and no error accumulation [1].

Many researchers suggested and analyzed parallel mechanisms for some decades. Hasselbach et al. have investigated several positioning platform based on parallel mechanism and emphasized the advantages of parallel mechanism in precision positioning field [2]. Choi et al. have suggested a novel 4-DOF parallel mechanism and designed dynamic controller for high accuracy tracking performance [3].

To overcome the trade-off between accuracy and stroke in actuation system, a dual stage servo system is proposed and researched [4]. Many researchers have also attempted to adopt the dual stage system to parallel mechanism. Takeda et al. have designed parallel manipulator platform based on the Stewart-Gough platform using dual stage actuation system [5]. Dong et al. designed 6-DOF parallel mechanism platform by using piezo electric actuators and piezo ceramic actuators [6].

The suggested mechanism by authors also adopts the dual stage servo system to realize long stroke and high accuracy, simultaneously. The mechanism has the advantage of rotational capability of 100 degree [7]. Among the coarse and fine actuators of dual stage system, the control of fine actuators is more important than that of the coarse actuators for realizing high speed and accuracy. The parallel mechanism platform also needs to be implemented effectively for the fine actuation system to get fast and accurate response. This paper presents a procedure for developing a controller that shows good performance for the fine actuation system.

The rest of the paper is organized as follows. In Section 2, the parallel mechanism and developed micro parallel positioning platform are described. Section 3 presents kinematic and dynamic modeling for controller synthesis. The unknown parameters were estimated through an experiment. Section 4 presents the synthesis of PID-based, mixed-sensitivity H_2 and H_∞ controllers, respectively. The response of fine actuation system was verified and compared with one another through extensive simulations and experiments and is discussed in Section 5. Conclusions are presented in Section 6.

II. MICRO PARALLEL POSITIONING PLATFORM

In this selection, the parallel mechanism and manufacturing of a 3-DOF micro parallel positioning platform is proposed.

A. Mechanism description

The micro parallel mechanism platform can realize 3-DOF motion. It can translate along the x- and y-axis and rotate for the α-axis (along the x-axis). The translational workspace is 5 mm × 5 mm and rotational workspace is 100 degree. The parallel mechanism is proposed in Fig. 1. The mechanism is composed of an end-effector, three links and a base platform. The base platform and end-effector are connected by two identical links and one parallelogram shaped link. The parallelogram shaped link can confine the rotation of end-effector so the end-effector only can be rotated for the α-axis.

The actuation part consists of two sets of linear actuators: coarse and fine actuation. Coarse actuation part shows relatively long stroke and rough accuracy and fine actuation part shows relatively short stroke and fine accuracy. So the combination of these two kinds of actuation can realize long stroke and fine accuracy. The coarse actuation part is designed vertically to enhance the mobility of the mechanism and the

fine actuation part is designed horizontally to increase the resolution of the mechanism [8].

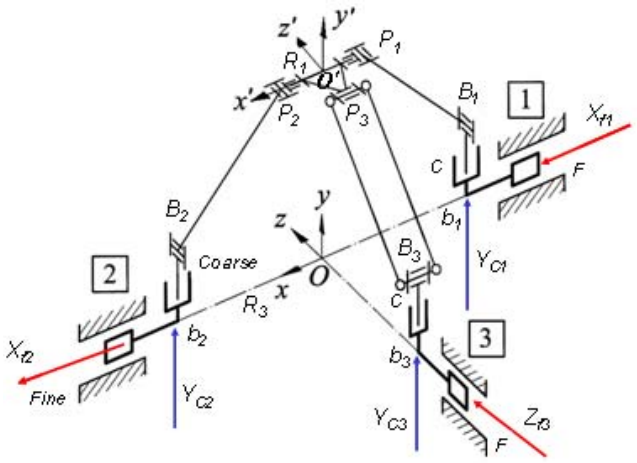

O-xyz = Fixed global reference frame
O'-x'y'a' = Movable top frame
P_1, P_2, P_3 = Movable platform joints
B_1, B_2, B_3 = Base joints
b_1, b_2, b_3 = Vectices of base plate
L or (P_iB_i) = Length of link for each legs
R_1 or ($O'P_i$) = Radius of moving platform
R_3 or (Ob_i) = Radius of base plate
Y_{C1}, Y_{C2}, Y_{C3} = Coarse actuator input displacements
X_{f1}, X_{f2}, Z_{f3} = Fine actuator input displacements

Figure 1. 3-DOF parallel mechanism and explanation of symbols

B. *Manufactured micro parallel positioning platform*

The micro positioning platform was manufactured and assembled. The overview of the platform is shown in Fig. 2. To measure the pose of the end-effector, sensing part is required. To measure the 3-DOF motion of end-effector, three linear scales are attached to the end-effector. The sensing part is shown in the left side of Fig. 2. At the bottom of Fig. 2, the tilting capability of the positioning platform is presented. Each photos show the tilting posture of the platform at -50, 0 and 50 degrees, respectively

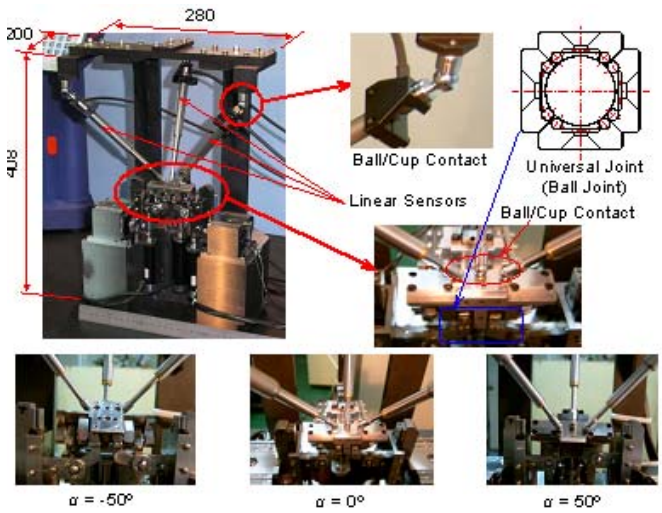

Figure 2. Manufactured micro parallel positioning platform

III. MODELING OF THE FINE ACTUATION SYSTEM

The first step of synthesizing a controller is modeling of the system. In this section, the modeling of the fine actuation system is presented.

A. *Constraint equation*

The kinematic constraint of the mechanism is that the length of each links is constant as shown in (1).

$$\| P_i - B_i \| = L \ , \text{where } i = 1, 2, 3 \tag{1}$$

Three scalar equations can be generated from (1) for the three links, respectively, as follows:

$$\left(x - R_1 + R_3 - X_{f1}\right)^2 + \left(y - Y_{c1}\right)^2 = L^2 \tag{2}$$

$$\left(x + R_1 - R_3 - X_{f2}\right)^2 + \left(y - Y_{c2}\right)^2 = L^2 \tag{3}$$

$$\left(-R_1\cos\alpha + R_3 - X_{f3}\right)^2 + x^2 + \left(R_1\sin\alpha + y - Y_{c3}\right)^2 = L^2 . \tag{4}$$

By using these constraints equation, the forward and inverse kinematics can be calculated.

B. *Jacobians*

Jacobian matrix is the relation of small perturbation of input and the response of output. By differentiating (2)-(4), we can get the equation in matrix form as follows:

$$J_p \delta p = J_q \delta q \tag{5}$$

where

$$J_q = \begin{bmatrix} x - R_1 + R_3 - X_{f1} & 0 & 0 \\ 0 & x + R_1 - R_3 + X_{f2} & 0 \\ 0 & 0 & -R_1\cos\alpha + R_3 - X_{f3} \end{bmatrix}$$

$$J_q = \begin{bmatrix} x - R_1 + R_3 - X_{f1} & 0 & 0 \\ 0 & x + R_1 - R_3 + X_{f2} & 0 \\ 0 & 0 & -R_1\cos\alpha + R_3 - X_{f3} \end{bmatrix}.$$

Then the Jacobian matrix of the fine actuation is defined as follows:

$$\delta p = J_f \delta q, \text{ where } J_f = J_p^{-1} J_q . \tag{6}$$

C. *Dynamic model*

The dynamic formulation is shown in Fig. 3. Each piezo actuators are assumed to be the mass-spring-damper system. The masses of links and end-effector are relatively lighter than the mass of each piezo actuation part, and so the masses are not included in the dynamic formulation. The dynamic equations for each piezo actuation parts are as follows:

$$F_i - k_i X_{fi} - c_i \dot{X}_{fi} = m_i \ddot{X}_{fi} . \tag{7}$$

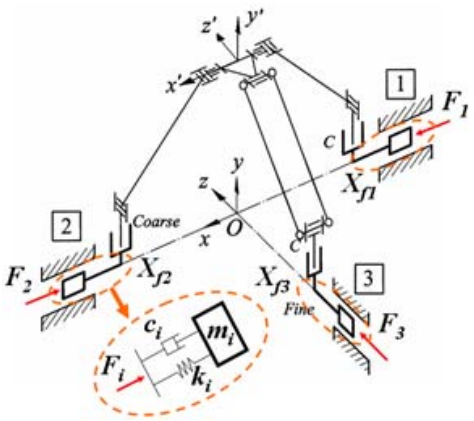

m_1, m_2, m_3 = Masses of fine actuation part
c_1, c_2, c_3 = damping coefficients of fine actuation part
k_1, k_2, k_3 = stiffness coefficients of fine actuation part
F_1, F_2, F_3 = Generated force from fine actuators
V_1, V_2, V_3 = Input voltage to fine actuators

Figure 3. Relation of force and dynamic response

By combining these independent dynamic equations and the Jacobian matrix (6) representing the geometric constraints, we can get the state-space dynamic model of the micro parallel positioning platform as follows:

$$\begin{aligned} \dot{x} &= Ax + Bu \\ y &= Cx \end{aligned} \tag{8}$$

where

$$x=[X_{f1}\ \dot{X}_{f1}\ X_{f2}\ \dot{X}_{f2}\ Z_{f3}\ \dot{Z}_{f3}]^{\mathrm{T}},\ u=[V_1\ V_2\ V_3]^{\mathrm{T}},\ y=[x\ y\ \alpha]^{\mathrm{T}}$$

$$A=\begin{bmatrix} 0 & 1 & 0 & 0 & 0 & 0 \\ -\frac{k_1}{m_1} & -\frac{c_1}{m_1} & 0 & 0 & 0 & 0 \\ 0 & 0 & 0 & 1 & 0 & 0 \\ 0 & 0 & -\frac{k_2}{m_2} & -\frac{c_2}{m_2} & 0 & 0 \\ 0 & 0 & 0 & 0 & 0 & 1 \\ 0 & 0 & 0 & 0 & -\frac{k_3}{m_3} & -\frac{c_3}{m_3} \end{bmatrix}, B=\begin{bmatrix} 0 & 0 & 0 \\ \frac{1}{m_1} & 0 & 0 \\ 0 & 0 & 0 \\ 0 & \frac{1}{m_2} & 0 \\ 0 & 0 & 0 \\ 0 & 0 & \frac{1}{m_3} \end{bmatrix} \times 10^{-3}$$

$$C=\begin{bmatrix} J_{f11} & 0 & J_{f12} & 0 & J_{f13} & 0 \\ J_{f21} & 0 & J_{f22} & 0 & J_{f23} & 0 \\ J_{f31} & 0 & J_{f32} & 0 & J_{f33} & 0 \end{bmatrix}.$$

We can calculate the Jacobian matrix and measure the mass of end-effector but we cannot calculate the stiffness and the damping coefficients. To apply this model to synthesize the controller, the proper stiffness and damping coefficient are required. In this research, the parameters were identified by experiments.

The process is shown in Fig. 4. To ignore the nonlinear property like backlash, we used the sinusoidal inputs of several frequencies instead of the white noise. Then we measured the magnitude change and phase delay of each sinusoidal input, and obtained the transfer relation which is indicated by a diamond shaped points of blue, red and magenta colors in Fig. 5.

Then, we adjusted the damping and stiffness coefficient and checked the bode plot of the transfer matrix to match the state-space model and experimental result. To simplify the dynamic model, we assume that the mass, damping and stiffness coefficient are the same value in each link, respectively. The estimated mass, damping and stiffness coefficient are presented in Table 1. The transfer matrix of the micro parallel positioning platform is shown in (9), and the frequency response of the model is shown as the solid lines in Fig. 5.

$$\begin{bmatrix} x \\ y \\ \alpha \end{bmatrix} = \begin{bmatrix} \frac{621.9}{s^2+406.1s+49750} & \frac{-621.9}{s^2+406.1s+49750} & 0 \\ \frac{510.4}{s^2+406.1s+49750} & \frac{510.4}{s^2+406.1s+49750} & \frac{161.7}{s^2+406.1s+49750} \\ \frac{-16.52}{s^2+406.1s+49750} & \frac{-16.52}{s^2+406.1s+49750} & \frac{50.05}{s^2+406.1s+49750} \end{bmatrix} \begin{bmatrix} V_1 \\ V_2 \\ V_3 \end{bmatrix} \tag{9}$$

The transfer matrix is composed of nine transfer functions. The transfer function from V_3 to x is assumed to be zero since the magnitude of the transfer function is relatively much lower than other transfer functions.

TABLE I. ESTIMATED COEFFICIENTS

Coefficient	m_i(kg)	c_i(N/μm·sec)	k_i(N/μm)
Value	0.804	0.00816	1.00

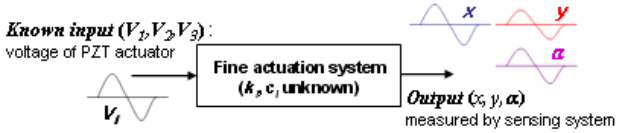

Figure 4. Experimental process of parameter estimation

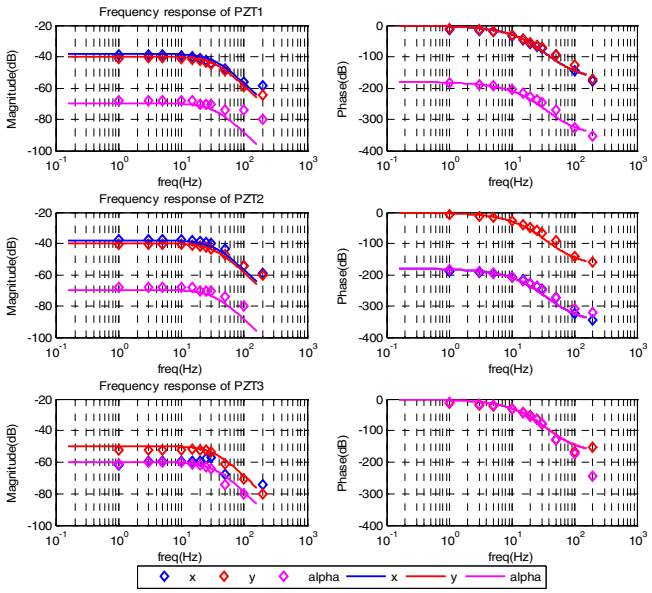

Figure 5. Frequency response of fine actuation system

IV. CONTROLLER SYNTHESIS

In this section, the synthesis procedures of PID-based, mixed-sensitivity H_2 and H_∞ controllers are presented.

A. *PID-based controller synthesis*

There are some applicable tuning rules for PID controller synthesis. In this paper, the optimal tuning rule suggested by Skogestad was adopted [9]. The tuning rule is simple and assures good closed-loop behavior.

To apply PID controller, decoupling matrix is required since PID controller should be designed based on single input single output system. For the decoupling matrix, we adopt the DC components of the inversing matrix of model matrix. Block diagram of the whole controller including decoupling matrix and PID controller is shown in Fig. 6.

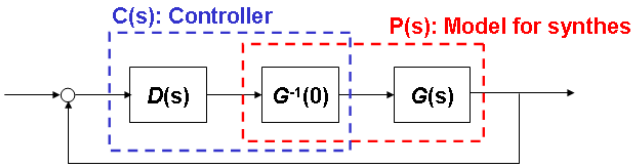

Figure 6. PID-based controller configuration

The resulting PID controller matrix, *D(s)* is designed as follows:

$$D(s) = \tilde{K}_c \frac{\tilde{\tau}_I s + 1}{\tilde{\tau}_I s} (\tilde{\tau}_D s + 1) \times I_{3\times 3} \tag{10}$$

where $\tilde{K}_c$, $\tilde{\tau}_I$, and $\tilde{\tau}_D$ are chosen as 7.47e0, 4.48e-3, and 4.48e-3, respectively. The stability is checked by the eigenvalues of the closed-loop system.

B. *Mixed-sensitivity H_2 and H_∞ controller synthesis*

The standard form to synthesize mixed-sensitivity H_2 and H_∞ controllers is shown in Fig. 7. The input/output relation of the standard form to follow the reference input can be expressed in matrix form as follows [10]:

$$\begin{bmatrix} z_1 \\ z_2 \\ z_3 \\ v \end{bmatrix} = \begin{bmatrix} 0 & W_u \\ 0 & W_T G_c \\ W_p & -W_p G_c \\ I & -G_c \end{bmatrix} \begin{bmatrix} r \\ u \end{bmatrix}. \tag{11}$$

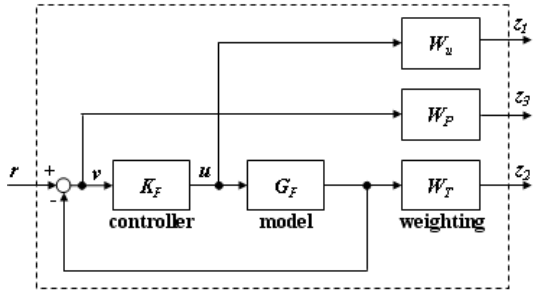

Figure 7. Standard form to synthesize mixed-sensitivity controllers

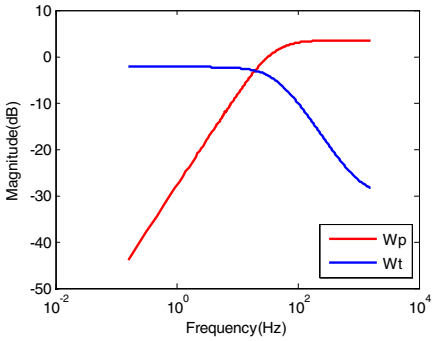

Figure 8. Magnitude plot of weighting matrices

The mixed-sensitivity H_2 and H_∞ controller synthesis problem is defined as a matrix optimization problem as in (12). The H_2 and H_∞ problem are divided by the type of objective function which is 2-norm or infinite norm.

$$\min_K \|N(K)\|, \quad N = \begin{bmatrix} W_u KS \\ W_T T \\ W_P S \end{bmatrix} \tag{12}$$
$$where\ S = (1+GK)^{-1}, T = GK(1+GK)^{-1}$$

The weighting matrices are designed to follow low frequency reference and to decrease high frequency disturbance. The resulting weighting matrices are defined in (13) and the magnitude plot is shown in Fig. 8. W_p is constructed to attenuate the disturbances in the low frequency region maximally up to -40 dB at 1 Hz and W_t is designed to guarantee the frequency band of 35 Hz. W_u is designed as a constant matrix.

$$W_p = \begin{bmatrix} \frac{0.667s+157}{s+0.01} & 0 & 0 \\ 0 & \frac{0.667s+157}{s+0.01} & 0 \\ 0 & 0 & \frac{0.4s+157}{s+0.01} \end{bmatrix}, \quad W_u = 10^{-3} I_{3\times 3}, \tag{13}$$
$$W_t = \begin{bmatrix} \frac{s+285}{0.0316s+219} & 0 & 0 \\ 0 & \frac{s+285}{0.0316s+219} & 0 \\ 0 & 0 & \frac{s+285}{0.0316s+219} \end{bmatrix}$$

By controller synthesis algorithms, H_2 and H_∞ controllers can be synthesized, respectively. Each controller is 4th-ordered controller. Bode plots of developed controllers are presented in Fig. 9, respectively.

V. SIMULATION AND EXPERIMENT

A. *Experimental set up*

The experimental set up is shown in Fig. 10. DS1103 control board (dSPACE) is used as the controller and three sets of PX38SG (Piezojena) are implemented as the fine actuators. The actuators are actuated by voltage of 0-10V. The response is measured by ST-3088 (Heidenhein) which is calibrated to guarantee submicron measuring accuracy.

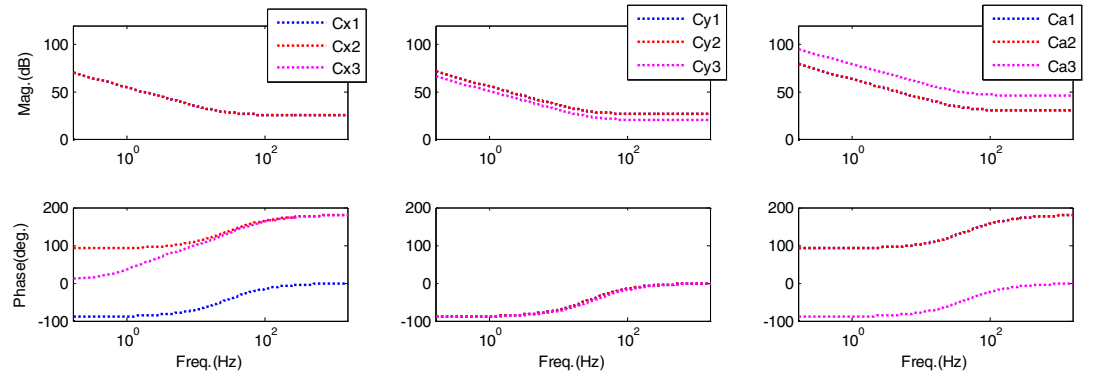

(a) Bode plot of H_2 controllers

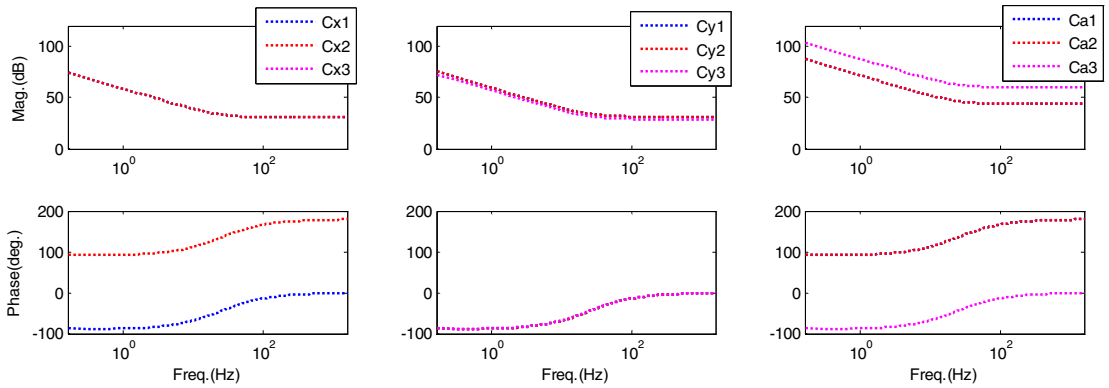

(b) Bode plot of H_∞ controllers

Figure 9. Bode plots of H_2 and H_∞ controllers

The performances of the PID-based, H_2, and H_∞ controller are verified and compared by step response simulation and experiment. 0.001mm and 0.002 degree steps in translational and rotational directions are applied, respectively.

In the simulation, the PID-based controller guarantees the stability. However, in the experiment, the PID-based controller shows unstable motion since it has closed-loop eigenvalue near the origin. It is also observed in the simulation that there is small resonance oscillation in the response, and so the simulation data is used to compare the response of controllers.

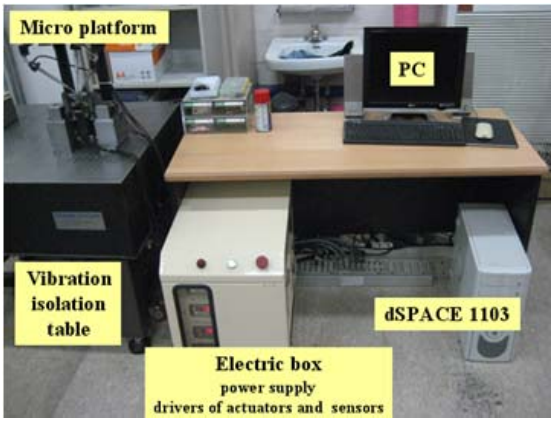

Figure 10. Experimental set up

The results of simulation and experiment are presented in Fig. 11. The top, middle and bottom figures show the response of PID-based controller, mixed-sensitivity H_2 controller and mixed-sensitivity H_∞ controller, respectively. The left, middle and right figures show the response in *x*-, *y*- and α-directional responses, respectively. The green lines present the experimental result and the lines of other colors present the result of simulation.

The overshoot and settling time of each controller are summarized in Table 2. The result of each controller is analyzed by smaller-the-better index as (12) where 10 % and 0.02 sec are selected from requirement of the performance:

$$Index = \frac{1}{6}\left(\sum_{x,y,\alpha}\frac{overshoot}{10} + \sum_{x,y,\alpha}\frac{settling\ time}{0.02}\right) \quad (12)$$

As a result, the PID-based controller shows relatively high overshoot and the H_2 controller shows relatively slow settling time. In conclusion, the H_∞ controller shows the best performance among the three candidates.

TABLE II. OVERSHOOT AND SETTLING TIME

type	Overshoot (%)			Settling time (sec)			Index
	x	*y*	*α*	*x*	*y*	*α*	
PID	20.27	19.30	15.27	0.016	0.016	0.014	1.289
H_2	0.785	1.167	1.915	0.022	0.026	0.048	0.852
H_∞	3.859	2.354	5.600	0.015	0.018	0.011	0.555

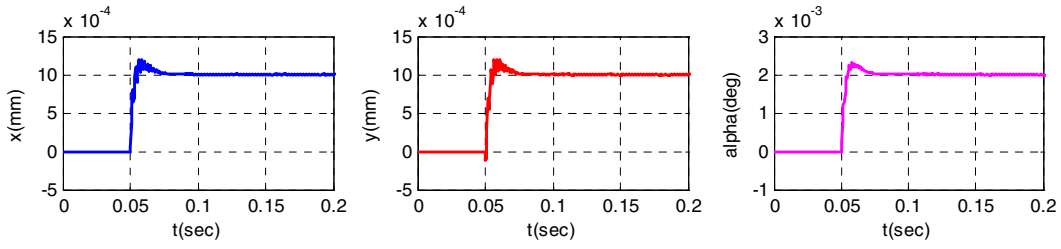

(a) Step response of PID controller

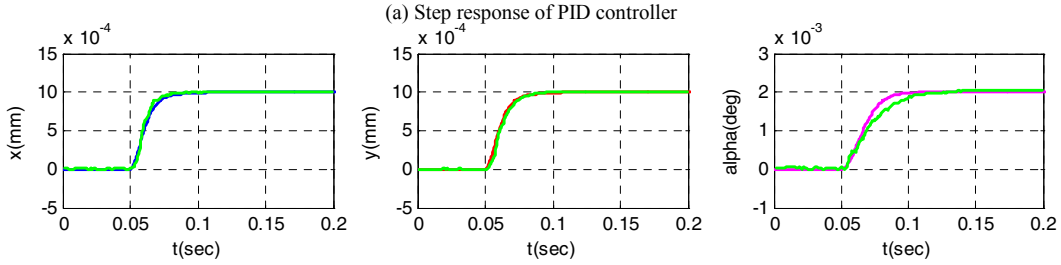

(b) Step response of mixed-sensitivity H_2 controller

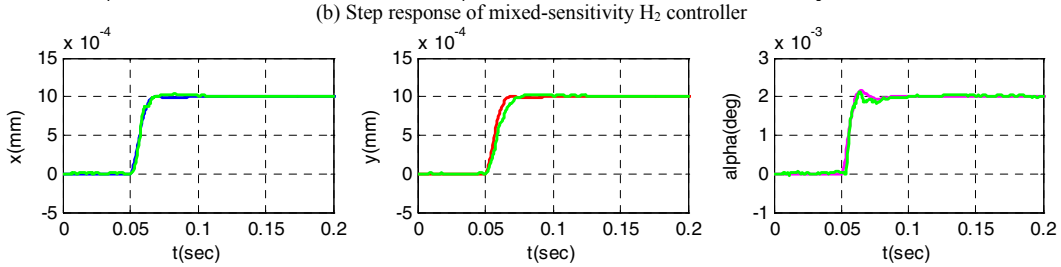

(c) Step response of mixed-sensitivity H_∞ controller

Figure 11. Step response of the each controller

The PID-based controller guarantees stability in the simulation stage, but the PID controller cannot guarantee stability since the controller has small stability margins comparing to the other robust controllers.

Based on the definition of the norm, H_2 controller is a controller that minimizes the 2-norm in the frequency domain and H_∞ controller is a controller that minimizes the L_2 gain in the time domain. Thus, in the tracking application, I believe H_∞ controller is more suitable controller than the H_2 controller.

VI. Conclusion

In this paper, the synthesis procedure for fine actuation system of 3-DOF micro parallel positioning platform is presented. First, the dynamic modeling was formulated based on the physics-based modeling, and the unknown parameters were estimated by system identification experiment. Based on the multi-input multi-output linear model, three kinds of controllers were synthesized and analyzed by simulation and experiment. As a result, the mixed-sensitivity H_∞ controller shows best performance in overshoot and settling time than the other two controllers. The developed controller will be integrated with the controller for coarse actuator to get both long stroke and high accuracy, simultaneously.

Acknowledgment

This work was sponsored by the Brain Korea 21 program and Engineering Research Center for Micro-thermal Systems.

References

[1] J.P. Merlet, Parallel robots, Springer, 2006.

[2] J. Hasselbach, J. Wreqe, A. Raatz, and O. Becker, “Aspects on design of high precision parallel robots,” Assembly Automation, vol. 24, no. 1, pp. 49-57, 2004.

[3] H. Choi, O. Company, F. Pierrot, A. Konno, T. Shibukawa and M. Uchiyama, “Design and control of a novel 4-DOFs parallel robot H4,” IEEE Interational Conference on Robotics and Automation, vol. 1, pp. 1185-90, 2003.

[4] S. Schroeck, W. Messner, and R. McNab, “On compensator design for linear time-invariant dual-input single-output systems,” IEEE/ASME Transactions on Mechatronics, vol. 6, no. 1, pp. 50-57, 2001.

[5] Y. Takeda, K. Ichikawa, H. Funabashi and K. Hirose, “An in-parallel actuated manipulator with redundant actuators for gross and fine motions,” IEEE International Conference on Robotics and Automation, 2003.

[6] W. Dong, L. Sun, and Z. Du, “Design of precision compliant positioner driven by dual piezoelectric actuators,” Sensors and Actuators A: Physical, vol. 135, no. 1, pp. 250-256, 2007.

[7] D. Kang, T. Seo, Y. Yoon, B. Shin, X. Liu, and J. Kim, “A micro-positioning parallel mechanism platform with 100-degree tilting capability,” Annals of the CIRP, vol. 55, no. 1, pp. 377-380, 2006.

[8] K. Oh, X. Liu, D. Kang, and J. Kim, “Optimal design of a micro parallel positioning platform. Part I: Kinematic analysis,” Robotica, vol. 22, pp. 599-609, 2004.

[9] S. Skogestad, “Simple analytic rules for model reduction and PID controller tuning,” Journal of Process Control, vol. 13, no. 4, pp. 291-309, 2003.

[10] S. Skogestad, and I. Postletwaite, Multivariable feedback control – Analysis and design, Chichester, UK: John Wiley & Sons, 1996.